Supplement of Atmos. Chem. Phys., 21, 15023–15063, 2021
https://doi.org/10.5194/acp-21-15023-2021-supplement

Atmospheric Chemistry and Physics
Open Access
EGU

Supplement of

Ambient aerosol properties in the remote atmosphere from global-scale in situ measurements

Charles A. Brock et al.

Correspondence to: Charles A. Brock (charles.a.brock@noaa.gov)

Four-mode lognormal fits to measured size distributions

Lognormal functions (Eq. 1) provide a concise description of the aerosol size distribution. Objectively fitting lognormal curves to multiple, dynamically varying modes spanning the diameter range from 3 nm to 50 μm is quite challenging. We have developed the following approach, which results in four lognormal functions that summed together accurately represent the number, surface, and volume of the entire size distribution. The coarse mode is first fitted using the portion of the volume size distribution with diameters from 1-6 μm, to avoid fitting noise from larger particles with poor counting statistics. The fitted mode diameter $D_{g,v}$ is constrained to lie between 1 and 10 μm, and the geometric standard deviation σ_g is constrained between 1.5 and 4. If the least-squares fit to Eq. 1 successfully converges, the volume median diameter is converted to number median diameter using the Hatch-Choate relationships (Heintzenberg, 1994) and the integrated volume converted to integrated number. This fitted coarse-mode lognormal function is then subtracted from the original size distribution. Negative residual values are set to zero. The residual size distribution is then converted to volume space, and a lognormal fit is made to particles with diameters from 0.08-1 μm, with constraints of $D_{g,v}$ from 0.1-1.2 μm and of σ_g from 1.2-2.5. As before, the fitted distribution is converted to number space and subtracted from the residual size distribution. The Aitken and nucleation modes are subsequently each fitted directly to the residual number size distribution with constraints of $D_{g,n}$ from 0.01-0.2 μm and of σ_g from 1.2-2.5 over the size range from 0.008-0.2 μm for the Aitken mode, and constraints of $D_{g,n}$ from 0.002-0.01 μm and of σ_g from 1.2-2.5 over the size range from 0.003 to 0.012 μm for the nucleation mode.

A reconstructed size distribution is created by summing the four lognormal functions from the four modes. The validity of the fits is checked by integrating the number, surface, and volume of this reconstructed size distribution and comparing it to the measured size distribution over different size ranges. Least-squares regressions of these integrated values from the lognormal fits and the measured size distributions are provided in Tables S2-4. Slopes lie between 0.94 and 1.08 with r^2 values >0.76.

Comparing mass from composition-resolved size distributions with AMS mass concentrations

The composition-resolved size distributions were calculated by mapping the composition measured by the AMS and the particle types measured by the PALMS onto the independently measured size distributions. The only quantitative compositional information the PALMS independently provides is the relative mass fractions of sulfate and organic material for the following non-refractory particle types: sulfate/organic (including unclassified particles), biomass burning, and meteoric. In contrast, the AMS directly measures the mass concentrations of OA and sulfate within the transmission window of its inlet, and this composition is applied to non-refractory particles with D_p<0.25 μm. However, for this combined dataset, only the relative abundance of the sulfate, OA, nitrate and chloride from the AMS and the sulfate and organic from the PALMS are used to determine the composition-resolved size distribution of non-refractory particles; their absolute concentrations derive primarily from the size distribution measurements.

To check the consistency of this mapping process, we compare the mass of sulfate and OA that can be integrated from the composition-resolved size distribution derived from the AMS, PALMS, and size distribution instruments with that directly measured with the AMS. This is accomplished as follows:

1) For particle types and sizes described by the AMS, which includes all particles with D_p<0.14 μm and the non-refractory particle types with D_p between 0.14 and 0.25 μm, the sulfate and OA mass fractions from the AMS measurements are used. The total mass of sulfate and OA is determined by integrating the volume size distribution and applying a density of 1.55 kg m^{-3} for the OA component and 1.75 kg m^{-3} for the sulfate and nitrate components, and 1.52 kg m^{-3} for the chloride component (Guo et al., 2021).

2) For the non-refractory particle types with Dp>0.25 μm, the PALMS-derived organic and sulfate mass fractions are applied, assuming no other components (e.g., nitrate) in the particles. Using the same densities as for the AMS, the total sulfate and OA can be integrated from the volume size distributions for the three non-refractory particle types.

3) Prior to integrating the size distributions in steps (1) and (2), a time-dependent AMS inlet transmission function (Guo et al., 2021) is applied. Thus the integrated OA and sulfate can be compared with the same values directly measured by the AMS instrument.

The sulfate and OA mass concentrations determined from this integration of the composition-resolved size distributions are plotted as a function of the directly-measured values from the AMS in Fig. S4. On the linear plots (Figs. S4a,b), a two-sided linear regression results in slopes of 1.18 for both and r2 values of 0.84 and 0.91, respectively. In the log-log plots with data points colored by GPS altitude (Figs. S4c,d), there is evidence of an altitude bias, with the sulfate and OA integrated from the composition-resolved size distributions biased low relative to the directly measured AMS values at high altitudes and vice versa at low altitudes. Overall, 90% of the calculated sulfate data points and 76% of the calculated OA data points were within a factor of the respective directly-measured AMS mass concentrations.

Table S1. Latitude boundaries for the regional air mass definitions for each ATom deployment.

Deployment	Arctic/midlatitude	North midlatitude/tropics	South midlatitude/tropics	Antarctic/midlatitude
ATom-1	60 °N	34 °N	21 °S	60 °S
ATom-2	60 °N	27 °N	32 °S	60 °S
ATom-3	61°N	29 °N	25 °S	60 °S
ATom-4	59 °N	20 °N	23 °S	60 °S

Table S2. Parameters from linear regression between integrated number concentration calculated from size distributions from four-mode lognormal fits to the measurements (ordinate) and integrated number directly from measurements (abscissa). Regression coefficients are from orthogonal distance (two-sided) regression. Pearson's regression coefficient (r^2) is shown. N is the number of 60s data points in the comparison.

Mode	Y-Intercept	Slope	r^2	N
Nucleation	-136 ± 5	0.979 ± 0.001	0.974	18742
Aitken	-93 ± 5	0.996 ± 0.003	0.761	18761
Accumulation	-9.9 ± 0.7	1.072 ± 0.002	0.939	18689
Coarse	0.036 ± 0.008	0.958 ± 0.002	0.905	18665

Table S3. As in Table S2, but for surface area.

Mode	Y-Intercept	Slope	r^2	N
Nucleation	-0.023 ± 0.001	0.977 ± 0.002	0.907	18742
Aitken	-0.29 ±-.01	0.990 ± 0.002	0.903	18761
Accumulation	-0.20 ± 0.04	1.037 ± 0.002	0.953	18689
Coarse	0.04 ± 0.09	0.991 ± 0.004	0.783	18665

Table S4. As in Table S2, but for volume.

Mode	Y-Intercept	Slope	r^2	N
Nucleation	1.8e-5 ± 2E-6	0.943 ± 0.003	0.836	18742
Aitken	-0.002 ± 0.0001	0.988 ± 0.002	0.920	18761
Accumulation	-0.0054± 0.002	1.030 ± 0.002	0.945	18689
Coarse	0.12± 0.03	1.022 ± 0.0)3	0.872	18665

Table S5. Total number of profiles/number of profiles meeting AOD criteria described in Sect. 2.8.

Region	ATom-1	ATom-2	ATom-3	ATom-4
Arctic	24/14	26/18	25/12	27/20
Pacific N. Midlatitude	9/7	31/22	33/20	35/26
Pacific Tropics	39/30	32/30	29/24	22/21
Pacific S. Midlatitudes	21/17	16/13	23/11	22/19
Antarctic/Southern Ocean	5/4	6/3	21/10	17/9
Atlantic S. Midlatitudes	10/10	4/3	11/10	17/11
Atlantic Tropics	17/16	16/12	20/17	15/15
Atlantic N. Midlatitudes	8/5	11/9	20/15	13/10

Table S6. BC mass mixing ratio (MMR; ng g^{-1}_{air}), number geometric mean diameter (D_g, nm) for BC core assuming mass-equivalent sphere, geometric standard deviation σ_g, thickness of non-absorbing coating (CT, nm) and calculated mass absorption cross section (MAC, m^2g^{-1}) at 532 nm for the different regions and air mass types. Data from the northern and southern hemisphere stratosphere have been combined.

Free Troposphere	**ATom-1**					**ATom-2**					**ATom-3**					**ATom-4**				
Pacific	**MMR**	**D_g**	**σ_g**	**CT**	**MAC**	**MMR**	**D_g**	**σ_g**	**CT**	**MAC**	**MMR**	**D_g**	**σ_g**	**CT**	**MAC**	**MMR**	**D_g**	**σ_g**	**CT**	**MAC**
Antarctic/S.Ocean	1.7	108	1.5	78	14.6	0.6	96	1.52	102	17.2	8.3	110	1.5	76	14.3	0.3	84	1.57	60	14.4
S. Midlatitudes	2	105	1.51	75	14.5	1.3	73	1.66	76	15.9	12.1	107	1.51	70	13.9	2	79	1.65	54	13.3
Tropics	2	91	1.58	58	13.3	2.6	94	1.6	81	14.6	4	96	1.53	61	13.9	0.9	76	1.63	64	14.8
N. Midlatitudes	9.9	83	1.62	72	14.9	9.3	97	1.63	102	14.9	9.3	84	1.65	71	14.2	18.8	84	1.6	65	14.4
Arctic	4.4	58	1.72	60	15.5	7.1	85	1.73	84	14.1	7.4	81	1.64	114	17.3	10.4	92	1.58	72	14.5
Atlantic																				
Antarctic/S.Ocean	–	–	–	–	–	–	–	–	–	–	2.4	115	1.49	77	14.0	0.3	87	1.63	66	13.7
S. Midlatitudes	3.5	106	1.52	67	13.6	0.2	102	1.52	85	15.4	7.9	98	1.58	61	12.9	0.9	93	1.54	51	13.1
Tropics	28.2	134	1.44	84	13.6	12.5	123	1.49	67	12.4	19.5	95	1.56	47	12.2	2.9	105	1.51	44	11.8
N. Midlatitudes	2.9	51	1.8	59	15.7	3.1	77	1.7	71	14.5	4.9	66	1.75	64	14.7	12.4	95	1.56	71	14.4
Arctic	2.7	63	1.74	83	16.9	4.3	75	1.7	73	14.9	7.7	62	1.82	75	15.8	11.8	98	1.53	76	15.0

Marine Boundary Layer																				
Pacific	**MMR**	**D_g**	**σ_g**	**CT**	**MAC**	**MMR**	**D_g**	**σ_g**	**CT**	**MAC**	**MMR**	**D_g**	**σ_g**	**CT**	**MAC**	**MMR**	**D_g**	**σ_g**	**CT**	**MAC**
Antarctic/S.Ocean	0.1	93[A]	1.6[A]	60[A]	13.0	0.1	93[A]	1.6[A]	60[A]	13.0	0.2	93[A]	1.6[A]	60[A]	13.0	0	93[A]	1.6[A]	60[A]	13.0
S. Midlatitudes	0.3	96	1.57	62	13.4	2.5	44	1.87	53	15.6	7.1	108	1.52	67	13.4	21.9	94	1.54	74	15.1
Tropics	13.1	98	1.53	58	13.4	3.5	106	1.54	84	14.6	9.6	112	1.48	65	13.6	17.6	98	1.54	61	13.5
N. Midlatitudes	1	93[A]	1.6[A]	60[A]	13.0	5.9	104	1.62	119	14.6	2.7	84	1.67	77	14.4	18.8	97	1.55	73	14.5
Arctic	0.5	93[A]	1.6[A]	60[A]	13.0	48.6	132	1.62	91	10.9	0.7	93[A]	1.6[A]	60[A]	13.0	6.7	95	1.6	60	12.7
Atlantic																				
Antarctic/S.Ocean	–	–	–	–	–	–	–	–	–	–	1.2	119	1.48	74	13.6		93[A]	1.6[A]	60[A]	13.0
S. Midlatitudes	42.7	122	1.47	57	12.1	0.3	93	1.6	52	12.3	20.7	90	1.61	44	11.7	0.5	93	1.6	57	12.7
Tropics	581.2	135	1.44	77	13.0	77.4	126	1.47	65	12.4	91.9	91	1.61	48	12.0	25	101	1.52	44	12.0
N. Midlatitudes	10.8	61	1.76	57	14.6	3	85	1.68	75	14.0	4.9	77	1.69	78	15.2	7.9	91	1.57	60	13.7
Arctic	0.7	38	2.06	101	20.8	7.9	107	1.54	81	14.2	0.4	93[A]	1.6[A]	60[A]	13.0	3.3	106	1.5	71	14.3

	MMR	**D_g**	**σ_g**	**CT**	**MAC**	**MMR**	**D_g**	**σ_g**	**CT**	**MAC**	**MMR**	**D_g**	**σ_g**	**CT**	**MAC**	**MMR**	**D_g**	**σ_g**	**CT**	**MAC**
Stratosphere	2	73	1.64	63	14.4	0.9	59	1.65	71	16.6	9.1	108	1.5	86	14.7	2.5	77	1.62	144	17.8
Biomass Burning Plumes	164.7	129	1.46	85	13.3	71.2	138	1.41	75	12.7	31.3	102	1.52	70	13.8	37.1	103	1.52	67	13.5
Dust Plumes	37.9	90	1.62	75	13.8	164.6	145	1.39	67	11.9	80.5	92	1.59	47	11.8	9.1	91	1.61	67	13.2

[A]Insufficient data for statistics; values are assumed.

Table S7. Lognormal parameters geometric standard deviation σ_g, number geometric mean diameter $D_{g,n}$, and volume geometric mean diameter $D_{g,v}$ for aerosol types from the OPAC database (Hess et al., 1998), from global shipborne data (Quinn et al., 2017), from the 7-mode modal aerosol model (MAM7; Liu et al., 2012), and from the ATom measurements. ATom values encompass the 25th to 75th percentiles; FT data are between 2 and 12 km. Quinn et al. data represent the full range. MAM7 ranges show the 10th and 90th percentiles. A subset of these data is shown in Fig. 15 of the main text.

Component	σ_g	$D_{g,n}$ (μm)	$D_{g,v}$ (μm)
Accumulation mode			
OPAC water-soluble	2.24	0.042	0.30
ATom N. Pac. FT accumulation mode	1.44-2.09	0.08-0.11	0.18-0.30
ATom BB accumulation mode	1.54-1.78	0.08-0.13	0.20-0.25
MAM7 accumulation mode	1.8	0.056-0.26	—
ATom N. Pac. FT Aitken mode	1.55-2.12	0.029-0.052	0.068-0.20
Aitken mode			
ATom MBL Aitken mode	1.57-1.89	0.029-0.047	0.065-0.14
Quinn et al. MBL Aitken mode	1.3-1.8	0.01-0.08	—
MAM7 Aitken mode	1.6	0.015-0.052	—
Black carbon			
OPAC soot	2.00	0.022	0.10
ATom free troposphere BC[1]	1.49-1.82	0.14-0.21	0.071[2]
ATom biomass burning BC[1]	1.41-1.52	0.17-0.20	0.074[2]
MAM7 primary carbon	1.6	0.039-0.13	—
Sea salt accumulation mode			
OPAC sea-salt accumulation mode[3]	2.03	0.42	1.9
ATom MBL accumulation mode[3]	1.32-1.53	0.13-0.18	0.21-0.25
Quinn et al. MBL accumulation mode	1.3-1.8	0.09-0.23	—
MAM7 fine sea-salt mode	2.0	0.095-0.56	—
Sea salt coarse mode			
OPAC sea-salt coarse mode	2.03	3.50	15.8
ATom MBL coarse mode	2.09-3.13	0.27-0.97	2.9-5.1
Quinn et al. MBL sea spray mode	2.2-2.8	0.17-0.45	—
MAM7 coarse sea-salt mode	2.0	0.63-3.7	—
Dust accumulation mode			
OPAC mineral accumulation mode[4]	2.00	0.78	3.20
ATom dust accumulation mode[4]	1.63-2.04	0.07-0.14	0.24-0.40
MAM7 fine dust mode	1.8	0.14-0.62	
Dust coarse mode			
OPAC mineral coarse mode	2.15	3.80	22.0
OPAC mineral-transported mode[5]	2.20	1.00	6.00
ATom dust coarse mode	1.77-2.01	0.88-1.09	2.7-4.1
MAM7 coarse dust mode	1.8	0.59-2.75	—

[1]Parameters for mass-equivalent sphere of uncoated BC
[2]Mean thickness of coating on BC
[3]A separate accumulation mode of sea-salt particles is not observed in the ATom dataset, but coarse-mode sea-salt particles extend into the accumulation mode. ATom modal parameters in the table are for the observed sulfate/organic-dominated accumulation mode.
[4]A separate accumulation mode of mineral particles is not observed in the ATom dataset. ATom modal parameters in the table are for the observed sulfate/organic-dominated accumulation mode.
[5]As described in Hess et al. (1998), "mineral-transported" refers to "desert dust that is transported over long distances with a reduced amount of large particles."

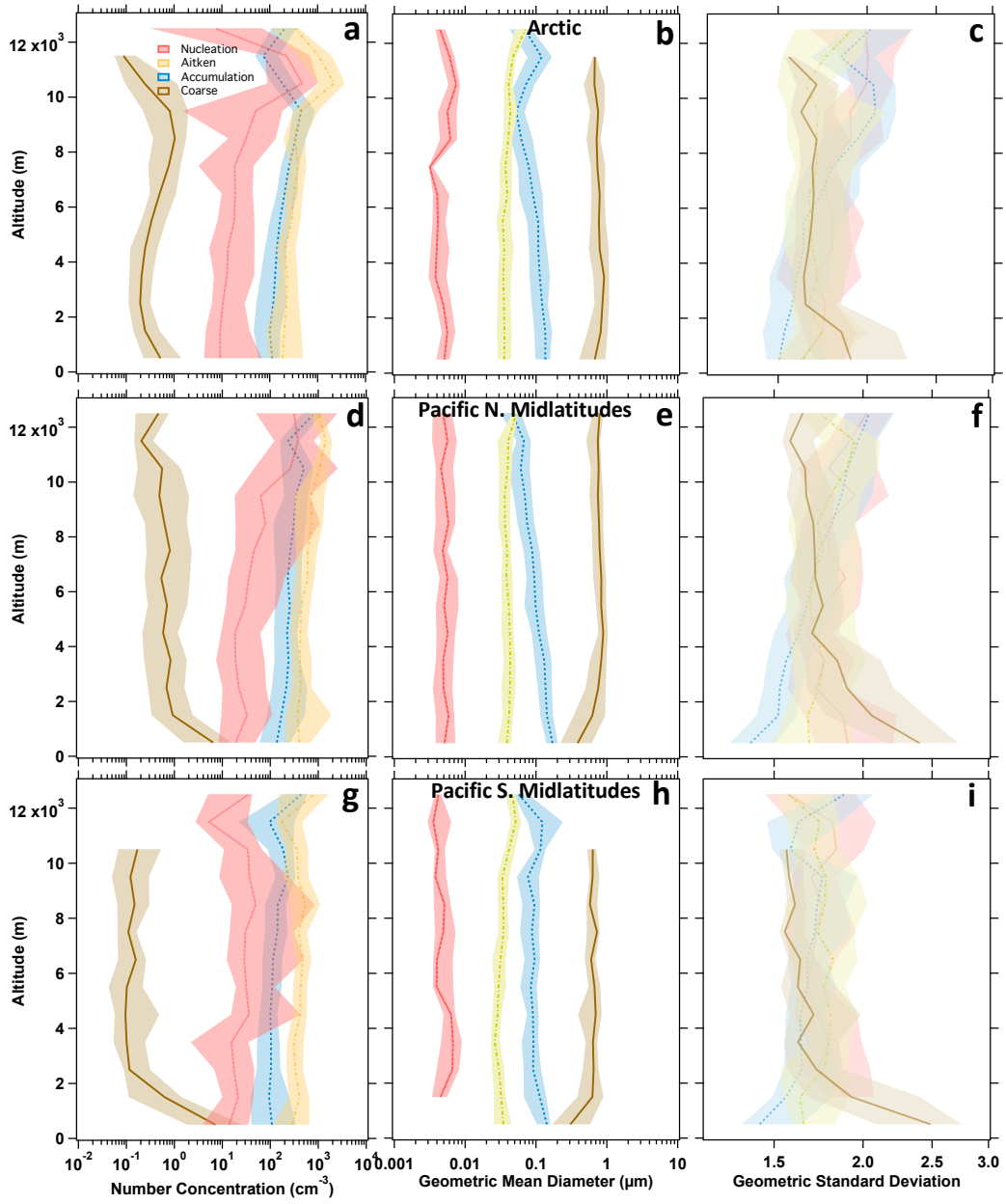

Figure S1. Vertical profiles of fitted lognormal parameters for the nucleation, Aitken, accumulation and coarse modes for the Arctic (a, b, and c), Pacific northern midlatitudes (d, e, and f), and the Pacific southern midlatitudes (g, h, and i) for the entire ATom project. Lines are median values and shaded regions show the interquartile range. Missing data in the coarse mode occur when concentrations were too low to provide adequate statistics for fitting. Similar vertical profiles for the tropics of the Pacific and Atlantic are in Fig. 12 of the main text.

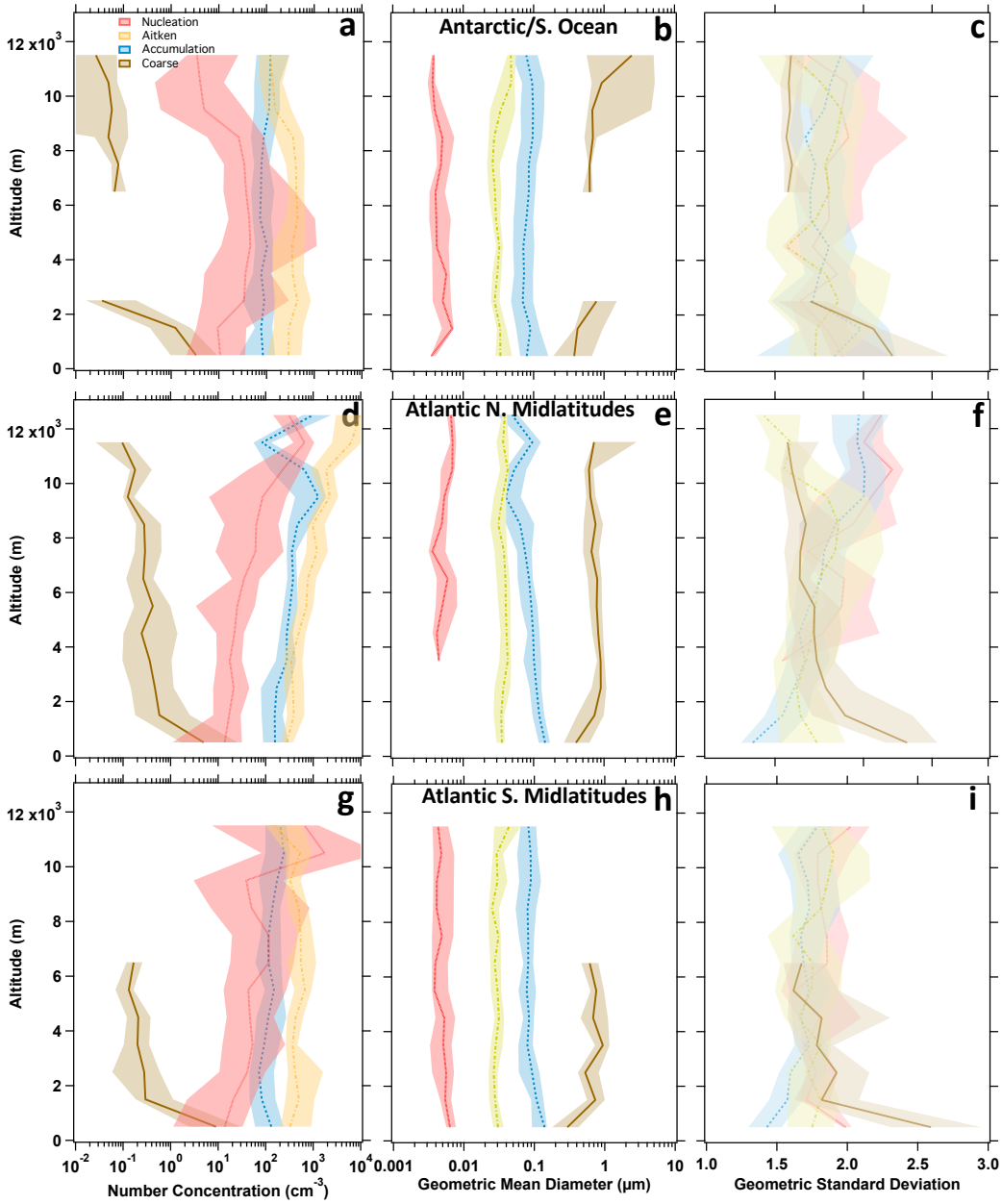

Figure S2. Vertical profiles of fitted lognormal parameters for the nucleation, Aitken, accumulation and coarse modes for the Antarctic and Southern Ocean (a, b, and c), Atlantic northern midlatitudes (d, e, and f), and the Atlantic southern midlatitudes (g, h, and i) for the entire ATom project. Lines are median values and shaded regions show the interquartile range. Missing data in the coarse mode occur when concentrations were too low to provide adequate statistics for fitting. Similar vertical profiles for the tropics of the Pacific and Atlantic are in Fig. 12 of the main text.

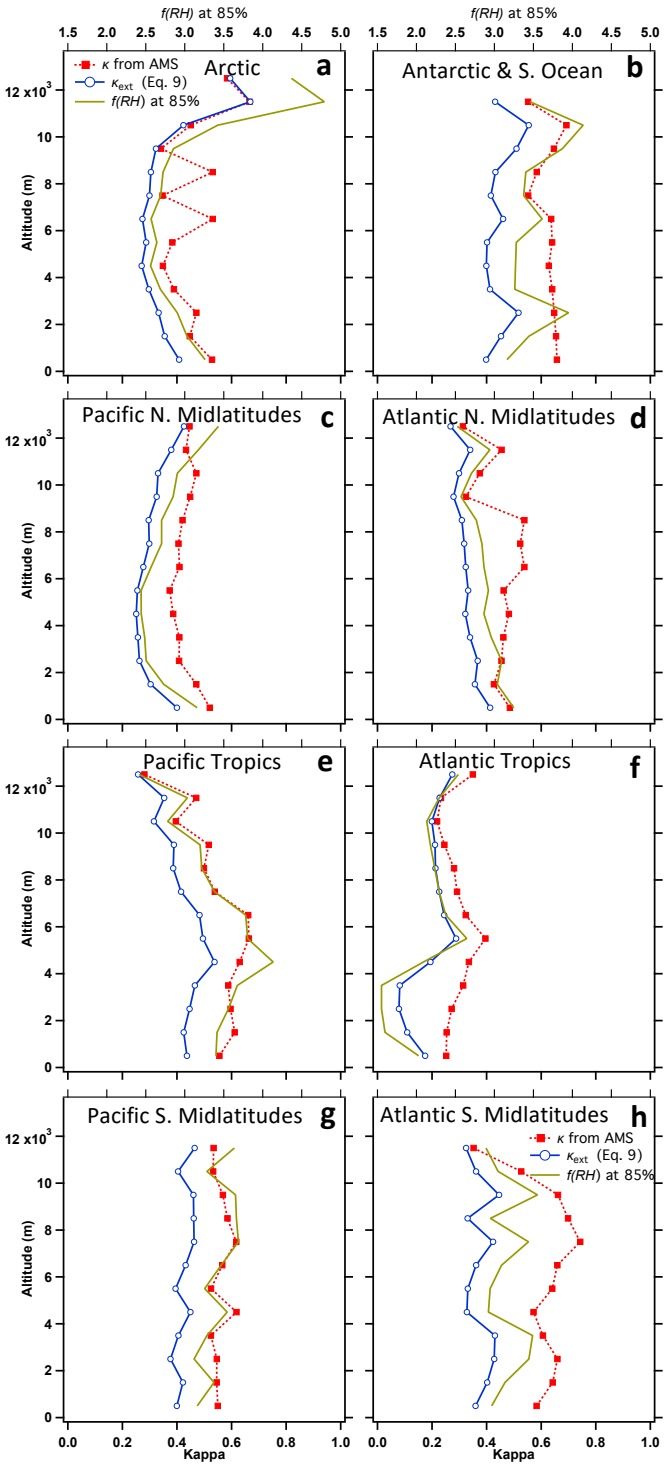

Figure S3. Median vertical profiles of κ determined from the AMS composition as described in Sect. 2.5 (bottom axis), of optical κ_{ext} values from Eq. 9 (bottom axis) and of *f(RH)* as described in Sect. 2.7.2 (top axis) for different regions sampled during the entire ATom project. a) Arctic. b) Antarctic and Southern Ocean. c) Pacific northern midlatitudes. d) Atlantic northern midlatitudes. e) Pacific tropics. f) Atlantic tropics. g) Pacific southern midlatitudes. h) Atlantic southern midlatitudes.

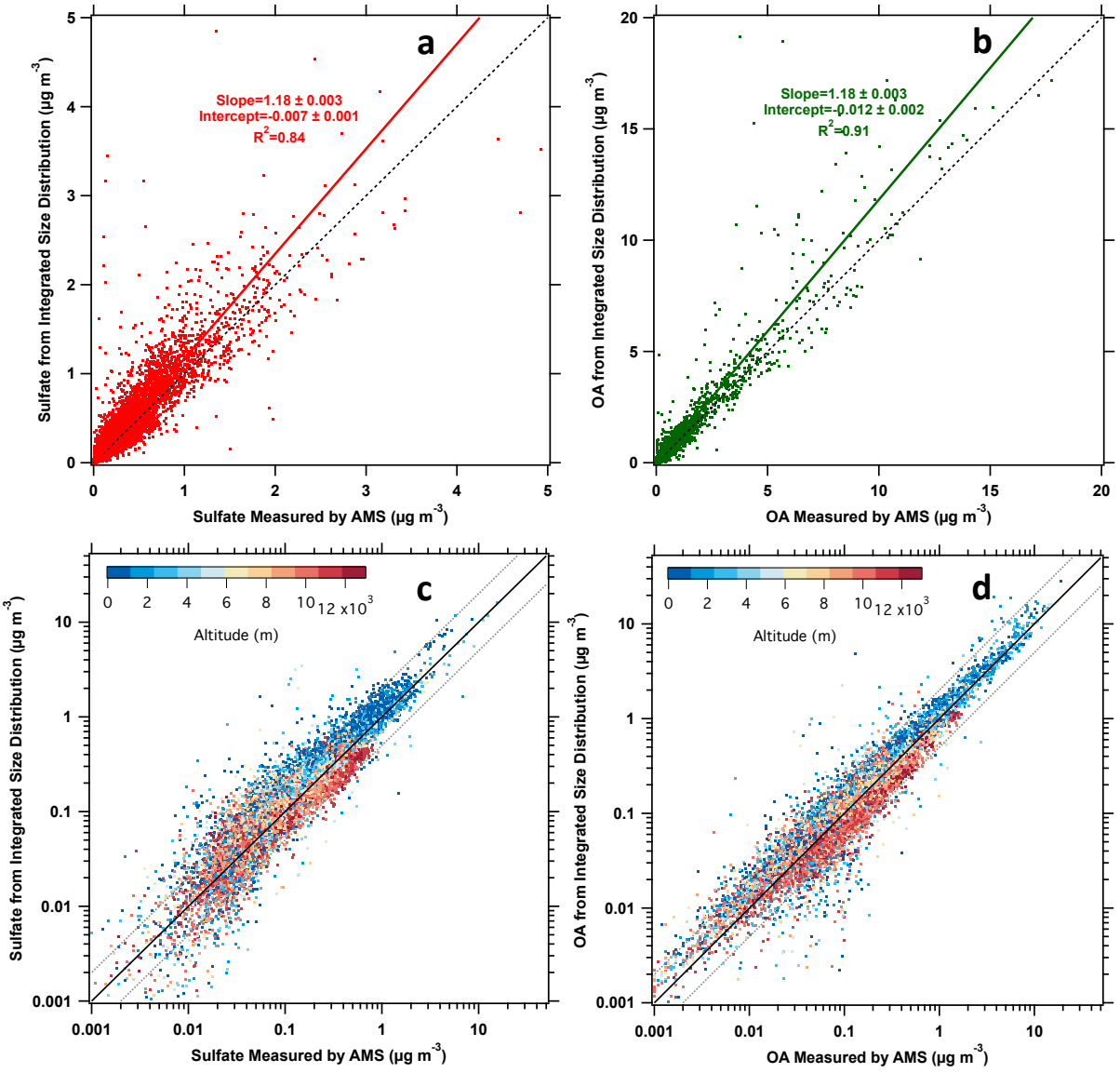

Figure S4. a) Sulfate calculated from integrating the composition-resolved size distributions over the transmission function of the AMS (Guo et al., 2020) as a function of sulfate directly measured by the AMS. Two sided linear regression (solid line) and 1:1 line (dashed line) are shown. b) As in (a), but for OA. c) As in (a), but a log-log plot colored by aircraft altitude. Solid line is 1:1 line and dashed lines are 2x and 0.5x the 1:1 line. d) As in (c), but for OA.

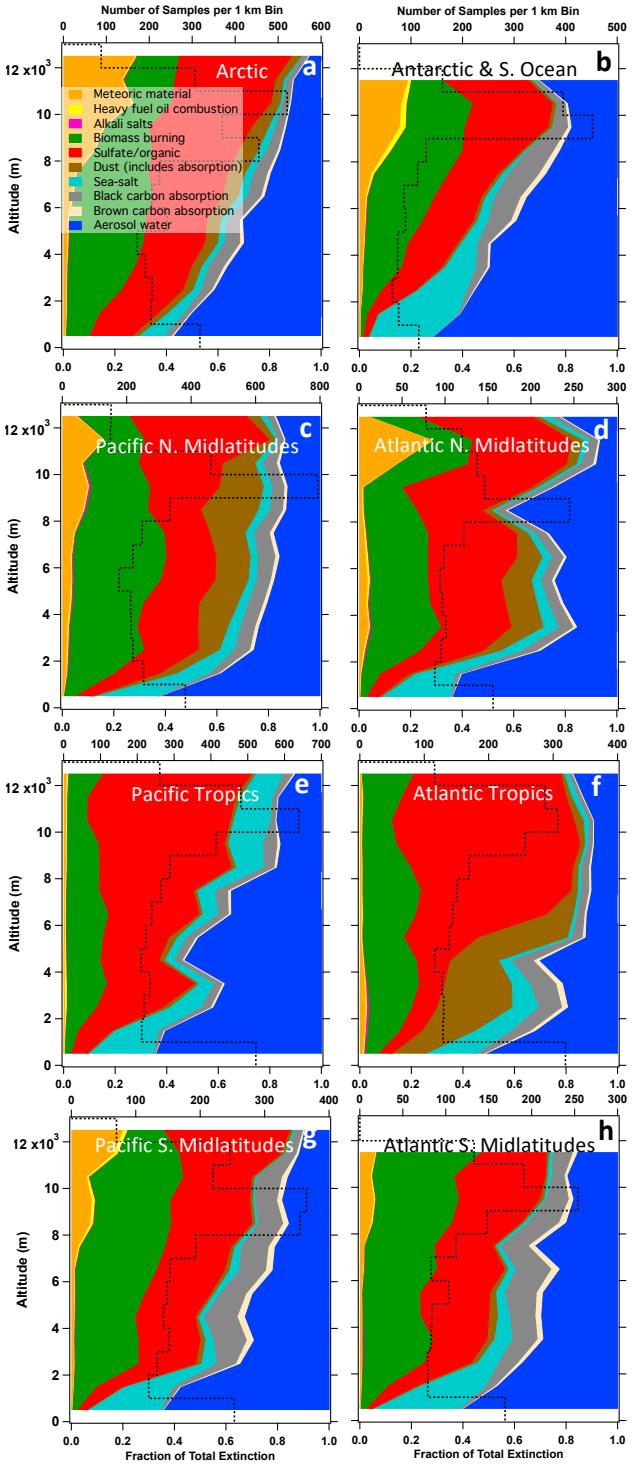

Figure S5. Vertical profiles of the fractional contribution to mean extinction (bottom axes) and the number of 60-s measurements in each 1-km altitude bin (dashed lines; top axes) from each of the aerosol types, for different regions, across all of the ATom deployments. Descriptions of the regions are given in Fig. 8 and Table S1. The mean extinction values contributed by each of the aerosol types are shown in the main text in Fig. 9.

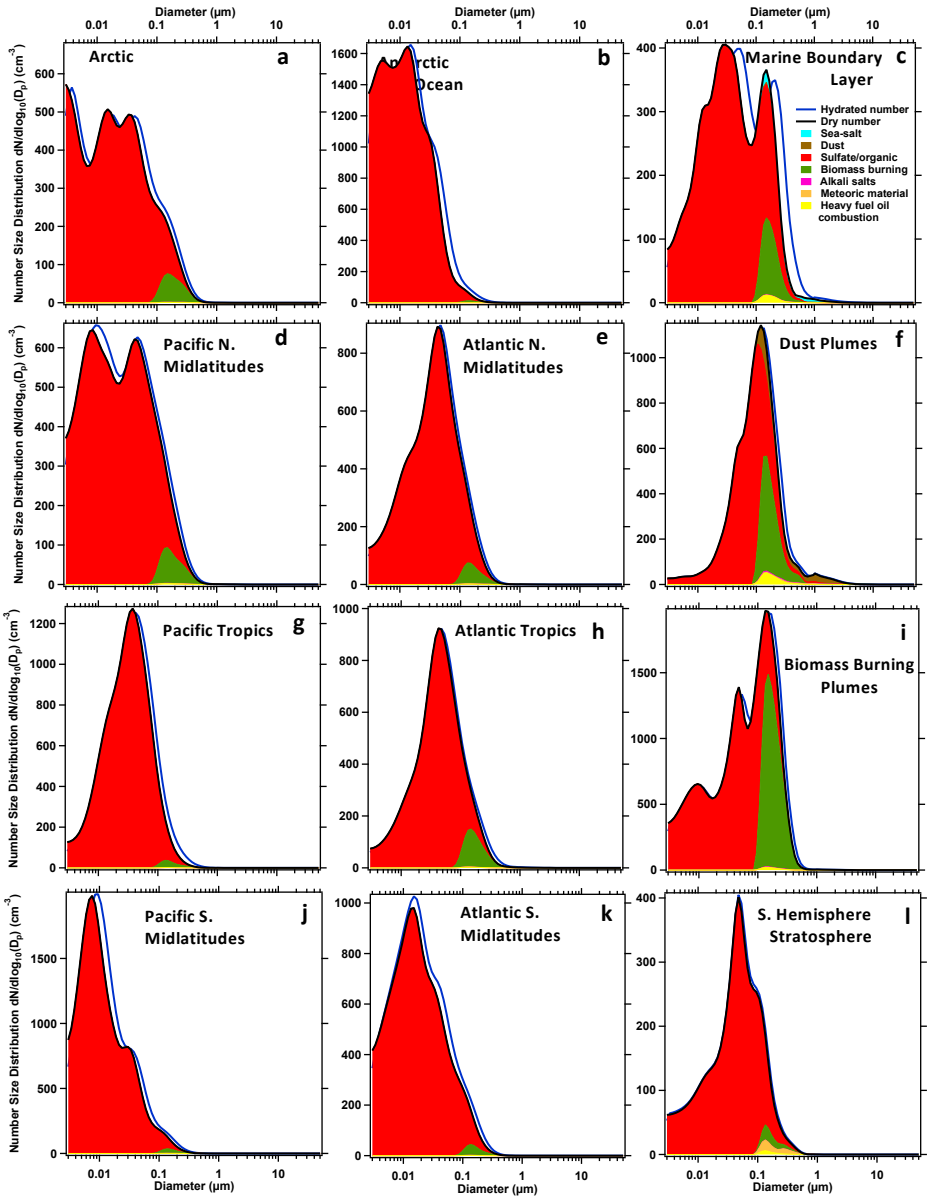

Figure S6. Number of particles of different aerosol types as a function of diameter, averaged over all data in different regions and air mass types across all of the ATom deployments. Note that scales on the y-axes vary. One pass of a binomial smoothing filter (Marchand and Marmet, 1983) has been applied to the data; PALMS particle types shown below 0.14 μm are extrapolated for smoothness. The volume size distributions are presented in Fig. 11 of the main text.

References

Heintzenberg, J. Properties of the log-normal particle size distribution, Aerosol Sci. Technol., 21, 46-48, https://doi.org/10.1080/02786829408959695, 1994.